

InterControl: Generate Human Motion Interactions by Controlling Every Joint

Zhenzhi Wang¹, Jingbo Wang², Dahua Lin^{1,2}, Bo Dai²

¹The Chinese University of Hong Kong, ²Shanghai Artificial Intelligence Laboratory

{wz122, wj020, dhlin}@ie.cuhk.edu.hk, daibo@pjlab.org.cn

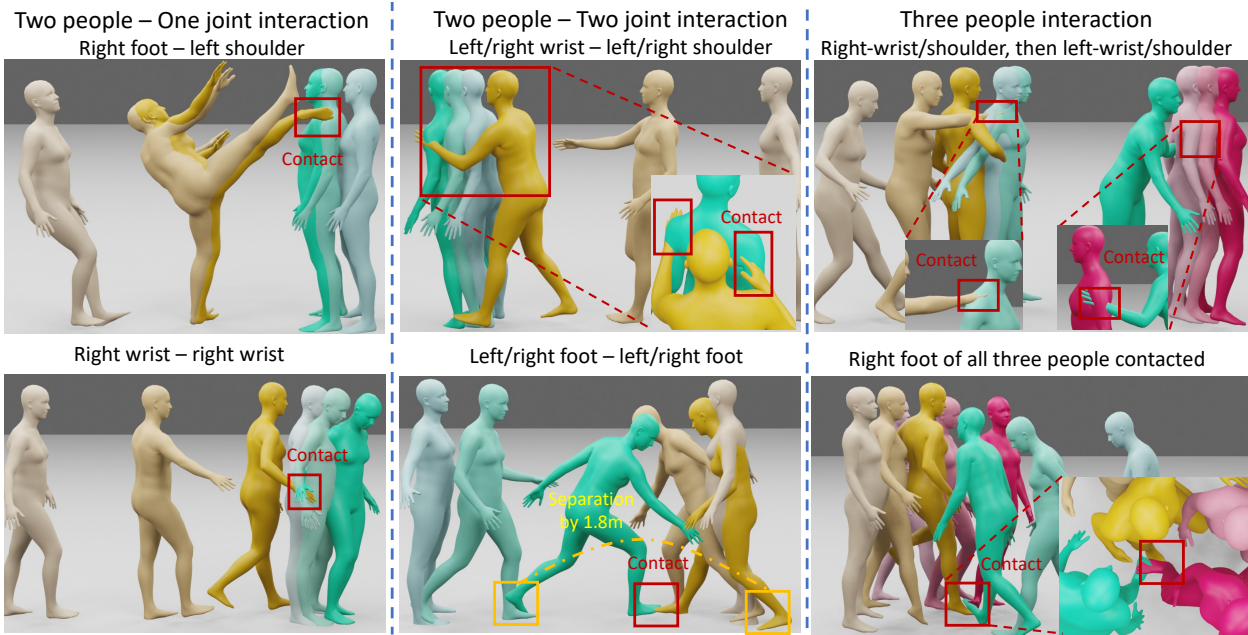


Figure 1. InterControl is able to generate **human interactions of arbitrary number** of people given joint-joint **contact** or **separation** pairs as spatial condition, and it is only trained on **single-person data**. Different colors are different people. Darker colors means later frames in a motion sequence. Penetrations of hands are due to motion data [13] only have wrists but no hands. Best viewed in color.

Abstract

Text-conditioned human motion generation model has achieved great progress by introducing diffusion models and corresponding control signals. However, the interaction between humans are still under explored. To model interactions of arbitrary number of humans, we define interactions as human joint pairs that are either in contact or separated, and leverage Large Language Model (LLM) Planner to translate interaction descriptions into contact plans. Based on the contact plans, interaction generation could be achieved by spatially controllable motion generation methods by taking joint contacts as spatial conditions. We present a novel approach named InterControl for flexible spatial control of every joint in every person at any time by leveraging motion diffusion model only trained on single-person data. We incorporate a motion control net to generate coherent and realistic motions given sparse

spatial control signals and a loss guidance module to precisely align any joint to the desired position in a classifier guidance manner via Inverse Kinematics (IK). Extensive experiments on HumanML3D and KIT-ML dataset demonstrate its effectiveness in versatile joint control. We also collect data of joint contact pairs by LLMs to show InterControl's ability in human interaction generation. Code is available at <https://github.com/zhenzhiwang/intercontrol>.

1. Introduction

Generating realistic and diverse human motions with controllable signals is a vital task in computer vision, as it has diverse applications in VR/AR, games, and films. In recent years, great progress has been achieved in human motion generation by introducing variational autoencoders (VAE) [29], Diffusion Models [21, 49] and large-scale lan-

guage models [4]. However, they are restricted to leverage control signals such as language prompts or action classes [5, 12–14, 41, 42, 51, 64], part of motion [9, 17, 51], or other related modalities [2, 16, 32, 33, 52], failing to perform flexible spatial control. Thus, they could only generate single-person motions conveying high-level semantics (e.g., texts) and are unable to generate **interactions** which requires *precise human joint control*. For example, two people’s hands should be contacted to generate the interaction ‘handshake’. This requires people’s hands to precisely reach the same location at the same time. Otherwise, there will be collisions or distances between hands.

This paper aims to explore an interaction generation paradigm that is generalizable to arbitrary number of humans for diverse group motion generation, instead of modeling the joint-distribution of fixed number of humans. Therefore, we resort to spatially controllable single-person motion generation and define *human interactions* as steps of *joint-joint contact pairs*. Inspired by human-scene interaction [58], we formulate interaction as joint contact pairs named *Chain of Contacts* (CoC) and translate language descriptions of group motions to be CoC by leveraging a Large Language Models (LLMs). By taking CoC as spatial conditions, we aims to generate versatile human interactions by controlling spatial relations of joints of a group of people. In this way, human interactions are annotation-free, and interactions could also involve multiple human joints.

As we could leverage joint-joint contact pairs generated by LLMs to generate interactions, the key challenges in modeling *interactions* is the *precise spatial control* in motion generation model. We found the difficulty have two main parts: (1) the discrepancy between *control signals in global space* and *relative motion representation* in mainstream datasets [13], and (2) the *sparsity* of control signals. As the semantics of human motions are independent of their locations in global space, previous works [13, 51] commonly utilize a relative motion representation to model human motions, where global positions could only be implicitly inferred by aggregating previous velocities. Although this representation makes the distribution of human motions easier to learn by neural networks, such discrepancy poses challenges to control local human poses with global position conditions, unlike image generation. Moreover, since control signals could be sparse in both joints and frames, the model needs to adaptively adjust trajectories in uncontrolled frames to satisfy the intermittent constraints.

Previous attempts in motion control [47, 51] exploit the inpainting ability of pretrained motion diffusion models by taking part of the motion as a condition. However, as the condition is in relative representation, they are still unable to control joints in global space. Besides, Guided Motion Diffusion (GMD) [25] proposes a two-stage diffusion model with root trajectory generation and local pose generation.

Although it manages to control root positions, spatially controlling *every joint at any time* is still infeasible. Thus, precise spatial joint control of any joints that is vital for interactions generation is still not solved.

In this paper, we propose InterControl, a novel human motion interaction generation method that is able to precisely control the position of any joint at any time for any person, and it is only trained on single-person motion data. As shown in Fig. 1, InterControl is able to generate interactions with one or two joints, or even interactions with more than two people. By adding spatial controls to a text-conditioned motion diffusion model (MDM) [51], InterControl is a unified framework of two types of spatial control modules: (1) *Motion ControlNet*: Inspired by ControlNet [63] in image generation, we utilize a Motion ControlNet that could be initialized from a pretrained MDM [51] and link an additional controlling branch to the original MDM via zero-initialized linear layers in an end-to-end manner. (2) *Loss Guidance*: To precisely align the global positions of generated motions with spatial conditions, we incorporate a loss guidance module to guide the denoising steps towards desired positions by optimizing distance measures via inverse kinematics (IK) [40]. It could be regarded as a classifier guidance [8], yet it has no extra classifiers to be trained and we utilize L-BFGS [35] instead of 1-st order gradients as the optimizer to better align joint position and save computations. In practice, Motion ControlNet is able to generate coherent and high-fidelity motions yet joint positions in global space are not perfect. Loss guidance is able to enforce the alignment of joints with desired positions yet it could lead to artifacts such as foot sliding and damage the learned motion distribution. With two complementary modules, InterControl is able to control multiple joints of any person at any time with only one model. Furthermore, InterControl is able to jointly optimize multiple types of spatial controls, such as orientation alignment, collision avoidance, and joint contacts, as long as the distance measures in loss guidance are differentiable. Extensive experiments in HumanML3D [13] and KIT-ML [43] datasets shows that InterControl outperforms state-of-the-art controllable motion generation methods by a large margin.

To summarize, our contributions are twofold: (1) InterControl is the first to perform precise spatial control of every joint in every person at any time, and enables controlling compositional human joints with only one model. (2) InterControl is the first to generate multi-person interactions with a single-person motion generation model in a zero-shot manner by leveraging the knowledge of LLMs.

2. Related Work

2.1. Human Motion Generation

Synthesizing human motions is a long-standing topic. Previous efforts integrate extensive multimodal data as condi-

tion to facilitate conditional human motion generation, including text [5, 13, 14, 28, 42, 51, 64], action label [12, 41], part of motion [9, 17, 51], music [32, 33, 52], speech [2, 16] and trajectory [25, 26, 45]. As texts are free-form information that convey rich semantics, recent progress in motion generation are mainly based on text conditions. For example, FLAME [28] introduces transformer [54] to process variable-length motion data and language description. MDM [51] introduces the diffusion model and uses classifier-free guidance for text-conditioned motion generation. MLD [5] further incorporates a VAE [29] to encode motions into vectors and makes the diffusion process in the latent space. Physdiff [61] integrates physical simulators as constraints in the diffusion process to make the generated motion physically plausible and reduce artifacts. PriorMDM [47] treats pretrained MDM [51] as a generative prior and controls MDM by motion inpainting. Our InterControl also use a pretrained MDM, yet we further train a Motion ControlNet instead of using inpainting. A concurrent work OmniControl [59] also incorporate classifier guidance [8] and controlnet [63] modules to control all joints in MDM, yet it focuses on single-person motion generation. We focus on generating multi-person interactions by effectively defining interactions as joint contact pairs and leveraging LLMs to generate contact plans. To execute contact plans, we incorporate spatial controls into motion generation models.

2.2. Human-related Interaction Generation.

As human motions could be affected or interacted by surrounding humans [27, 53, 65], objects [11, 24, 31, 50, 60] and scenes [18, 55–58, 66], generating interactions is also an important topic. Previous kinematics-based interaction generation methods are mainly about human-scene/object interaction. For example, Interdiff [60] uses the contact point of human joints and objects as the root to generate object motions. UniHSI [58] exploits LLM to generate contact steps between human joints and scene parts as an action plan and control the agent perform the plan via reinforcement learning. Previous human-human interaction methods are mostly physics-based and could only perform basic actions. To the best of our knowledge, we are the first to introduce text-conditioned human motion generation model to enable human-human interactions with rich semantics by controlling diverse human joints.

2.3. Controllable Diffusion Models

Diffusion-based generative models have achieved great progress in generating various modalities, such as image [8, 20, 46, 49], video [10, 15, 22] and audio [30]. Conditions and controlling ability in diffusion models are also well studied: (1) Inpainting-based methods [6, 7] predict part of the data with the observed parts as condition and rely on diffusion model to generate consistent output, which is

used in PriorMDM [47]. (2) Classifier-guidance [8] trains a separate classifier and exploits the gradient of classifier to guide the diffusion process. Our InterControl inherits the spirit of classifier-guidance, yet our guidance is provided by Inverse Kinematics (IK) and no classifier is needed. (3) Classifier-free guidance [20] trains a conditional and an unconditional diffusion model simultaneously and trade-off its quality and diversity by setting weights. (4) ControlNet [63] introduces a trainable copy of pretrained diffusion model to process the condition and freezes the original model to avoid degeneration of generation ability. It enables diverse types of dense control signals for various purpose with minimal finetuning effort. Our InterControl also incorporate the idea of ControlNet [63] to finetune the pretrained MDM [51] to process spatial control signals and imporve the quality of generated motions after joint control.

3. InterControl

InterControl aims to precisely control every joint of every person at any time for interaction generation, conditioned on text prompts and joint relations. To generate interactions with an arbitrary number of people, we develop control modules for a single-person motion diffusion model in Fig. 2, instead of modeling the joint-distribution of a fixed number of humans. Specifically, we define interactions as joint contact pairs and formulate interaction generation as spatially controllable motion generation by leveraging a LLM in Sec. 3.1. We finetune MDM [51] by ControlNet [63] to generate coherent and high-quality motions given spatial control signals in Sec. 3.3. As ControlNet alone could not precisely align joints and control signals, we design a loss guidance module to guide joints to desired positions with Inverse Kinematics (IK) in denoising steps in Sec. 3.4. Then, we show details to generate interactions from a single-person motion generation model in Sec. 3.5.

3.1. Formulation of Interaction Generation

Inspired by human-scene interaction [58], we define human interactions as Chain of Contacts $\mathcal{C} = \{\mathcal{S}_1, \mathcal{S}_2, \dots\}$, where \mathcal{S}_i is the i^{th} contact step. Taking two-person interaction as an example, each step \mathcal{S} has several contact pairs $\mathcal{S} = \{\{j_1^1, j_1^2, t_1^s, t_1^e, c_1, d_1\}, \{j_2^1, j_2^2, t_2^s, t_2^e, c_2, d_2\}, \dots\}$, where j_k^1 is the joint of person 1, j_k^2 is the joint of person 2, t_k^s and t_k^e means the start and end frame of the interaction, c_k means contact type from {contact, avoid} to pull or push, d_k is the desired distance in the interaction. By converting the contact pairs \mathcal{S} to the mask \mathbf{m} and distance d , and taking others' joint positions as condition, we could guide the multi-person motion generation process to have interactions between joints in the form of spatial distance. In this way, interaction generation is transformed to controllable human motion generation in our paradigm. Given

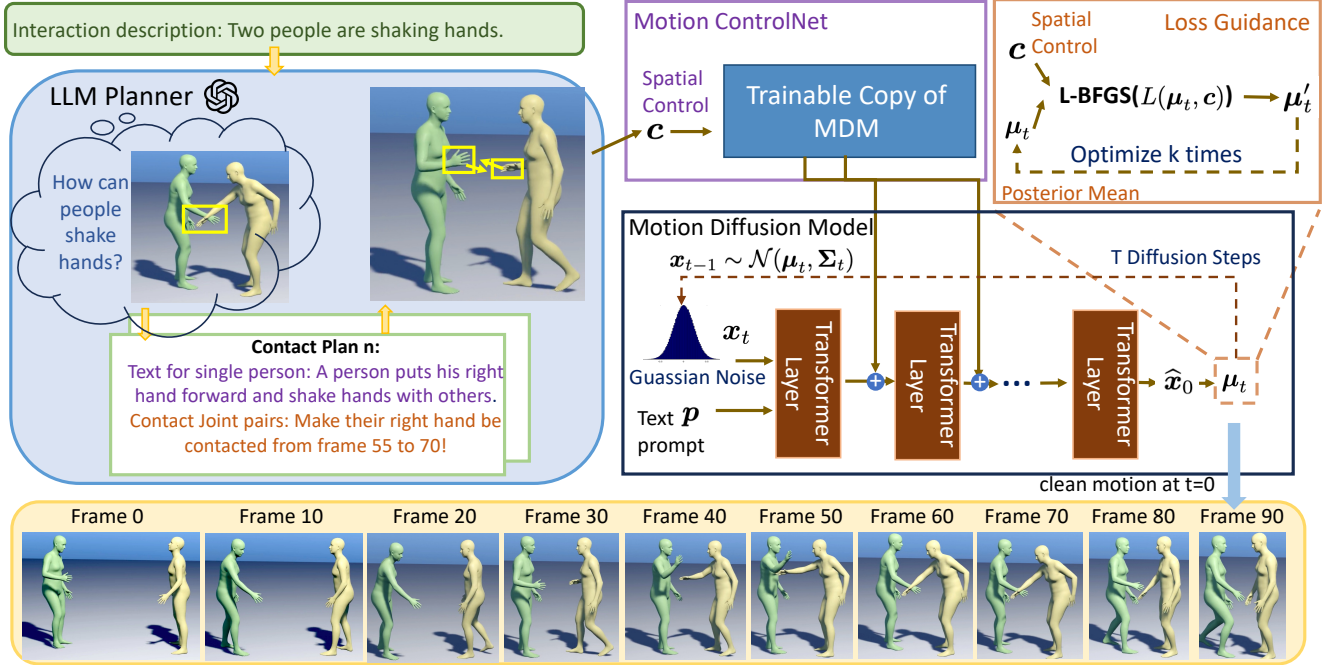


Figure 2. **Overview of our InterControl.** Our model could precisely control human joints in the global space for motion diffusion model via Motion ControlNet and Loss Guidance module. By leveraging LLM to construct plans of joint contact pairs for human interaction descriptions, our InterControl could generate multiple people’s interaction via a single-person motion generation model in a zero-shot manner. Penetrations of hands are due to motion data [13] only have wrists but no hands, so we set distance for wrists.

a text prompt p and a spatial control signal $c \in \mathbb{R}^{N \times J \times 3}$, controllable human motion generation aims to generate a motion sequence $x \in \mathbb{R}^{N \times D}$ whose joints in the global space is aligned with spatial control c . N is number of frames, J is number of joints (e.g., 22 in SMPL [36]), and D is the dimension of relative joint representations (e.g., 263 in HumanML3D [13]). It is non-trivial to incorporate spatial control in motion generation due to the discrepancy between the relative x and global c .

3.2. Human Motion Diffusion Model (MDM)

Relative Motion Representation. HumanML3D [13] dataset proposes a widely-used [5, 47, 51, 61] relative data representation, and is proved to be easier to learn realistic human motions. It consists of root joint velocity, other joints’ positions, velocities and rotations in the root space, and foot contact labels. It makes sense because the semantics of human motion is independent of global positions. To convert to global space, root velocities are aggregated, then other joints will be computed based on root. Please refer to Sec. 5 of HumanML3D [13] for details.

Due to such discrepancy of representations, previous inpainting-based methods [47, 51] struggles to control MDM. GMD [25] tried to solve this by decoupling motion generation to generation of root trajectory and pose, yet it can only control root joint. Directly adopting global joint positions to generate motions yields unnatural human poses such as unrealistic joint velocities and limb lengths.

Diffusion Process in MDM. Motivated by the success of image diffusion models [8, 20, 46, 49, 63], Motion Diffusion Model (MDM) [51] is proposed to synthesize sequence-level human motions conditioned on texts p via classifier-free guidance [20]. The diffusion process is modeled as a noising Markov process $q(x_t | x_{t-1}) = \mathcal{N}(\sqrt{\alpha_t}x_{t-1}, (1 - \alpha_t)\mathbf{I})$, where $\alpha_t \in (0, 1)$ are small constant hyper-parameters, thus $x_T \sim \mathcal{N}(0, \mathbf{I})$ if α_t is small enough. Here $x_t \in \mathbb{R}^{N \times D}$ is the entire motion sequence at denoising time-step t , and there are T time-steps in total. Thus, x_0 is the clean motion sequence, and x_T is almost a random noise to be sampled. The denoising Markov process is defined as $p_\theta(x_{t-1} | x_t, p) = \mathcal{N}(\mu_\theta(x_t, t, p), (1 - \alpha_t)\mathbf{I})$, where $\mu_\theta(x_t, t, p)$ is the estimated posterior mean for the $t - 1$ step from a neural network based on the input x_t and θ is its parameters. Following MDM, we predict the clean motion $x_0(x_t, t, p; \theta)$ instead of the noise ϵ via a transformer [54], and the posterior mean $\mu_\theta(x_t, t, p)$ is

$$\mu_\theta(x_t, t, p) = \frac{\sqrt{\bar{\alpha}_{t-1}}\beta_t}{1 - \bar{\alpha}_t}x_0(x_t, t, p; \theta) + \frac{\sqrt{\alpha_t}(1 - \bar{\alpha}_{t-1})}{1 - \bar{\alpha}_t}x_t, \quad (1)$$

where $\beta_t = 1 - \alpha_t$ and $\bar{\alpha}_t = \prod_{s=0}^t \alpha_s$. The network parameter θ of MDM is trained by minimizing the ℓ_2 -loss $\|x_0(x_t, t, p; \theta) - x_0^*\|_2^2$ where x_0^* is the ground-truth motion sequence and $x_0(x_t, t, p; \theta)$ is MDM’s prediction of x_0 at denoising time-step t .

3.3. Motion ControlNet for MDM

MDM is only conditioned on text prompt p . We further finetune it to process additional spatial conditions c . It is very challenging to deal with spatial conditions c as it could be **sparse** in both temporal and joint dimensions: (1) The number of joints we want to control could be small compared to the total number of joints, thus the model needs to adaptively adjust the position of other joints to make the entire motion sequence be realistic. (2) The frames we impose the joint control could be sparse, thus the model needs to fill-in natural human motions within frames without controls, including the root positions and human poses.

Inspired by ControlNet [63], we design a Motion ControlNet to adaptively generate realistic and high-fidelity motion sequences based on condition c . Motion ControlNet is a trainable copy of MDM, while MDM is frozen in our training process. Each transformer encoder layer of ControlNet and the original MDM is connected by a zero-initialized linear layer. So InterControl starts training from weights that is equivalent to a pretrained MDM and learns a residual feature for c in each layer via back-propagation. To process c , the uncontrolled joints, frames, and XYZ-dim are masked as 0. We find that the vanilla $c \in \mathbb{R}^{N \times 3J}$ is effective enough to control the pelvis (root) joint, yet it is still sub-optimal for other joints. Thus, we design a relative condition indicating the distance from the current positions of each joint to c . Suppose $R(\cdot)$ is a forward kinematics (FK) to convert relative motion $x \in \mathbb{R}^{N \times D}$ to global space $R(x) \in \mathbb{R}^{N \times J \times 3}$, the relative condition is $c' = c - R(x)$. To provide additional clues, we also use $c'' = c - R(x)^{root}$ to represent the distance from the current root to the desired position. We also use the normal of triangles (pelvis, left/right shoulder) n^s and (pelvis, left/right hip) n^h to represent the current orientation of human. The final condition to be fed to ControlNet is $c^{final} = cat(c', c'', n^s, n^h)$, where cat is concatenation. Please refer to Appendix A.2 for details of ControlNet’s architecture.

3.4. Loss Guidance via Inverse Kinematics

Although Motion ControlNet is able to adaptively adjust all joints’ positions based on sparse conditions, we find that the alignment between the predicted pose and the condition in global space is not precise. As Inverse Kinematics (IK) is a standard technique in optimizing joint rotations to reach desired global positions, we resort to it for guiding the diffusion process towards spatial conditions at test time in a classifier guidance [8] manner, which is called loss guidance.

Loss Guidance. Inspired by classifier guidance [8] and loss-guided diffusion [48], we use loss functions in the global space to guide the diffusion process in the denoising steps. Loss guidance accepts general forms of distance measurements, therefore it could both minimize it or

maximize it, leading to flexible control of joint relations (i.e., pull or push) in interactions. Taking global position $c \in \mathbb{R}^{N \times J \times 3}$, the distance between a joint and condition is $d_{nj} = \|c_{nj} - R(\mu_t)_{nj}\|_2$, where μ_t is short for $\mu_\theta(x_t, t, p)$ mentioned in Sec. 3.2, and $R(\cdot)$ is forward kinematics (FK). To allow the interaction of joints with some given distances $d' \in \mathbb{R}^{N \times J \times 3}$, loss of one joint is $l_{nj} = \text{ReLU}(d_{nj} - d'_{nj})$ to make the joint and condition be **contacted** within distance d'_{nj} ; and it is $l_{nj} = \text{ReLU}(d'_{nj} - d_{nj})$ to make the joint and condition be **far away**, where ReLU is a function to keep values ≥ 0 and set values ≤ 0 to 0. Finally, with a binary mask $m \in \{0, 1\}^{N \times J \times 3}$, the total loss for all joints and frames is

$$L(\mu_t, c) = \frac{\sum_n \sum_j m_{nj} \cdot l_{nj}}{\sum_n \sum_j m_{nj}}, \quad (2)$$

As ℓ_2 -loss and FK is high-order differentiable, we optimize $L(\mu_t, c)$ in Equ. 2 w.r.t μ_t by a 2nd-order optimizer L-BFGS [35] widely adopted in Inverse Kinematics, instead of 1st-order gradient. Classifier guidance [8] trains an image classifier and uses the gradient from the classification loss $\nabla_{x_t} \log f_\phi(y | x_t)$ to guide the diffusion process towards desired image class, where f_ϕ is the classifier, y is image class. However, we don’t have a huge neural network as the classifier in our framework. L-BFGS performs better in global position alignment and shows faster speed than 1st-order gradients. At each denoising step, we use L-BFGS to update posterior mean μ_t for k times, which k is a hyper-parameter. In the optimization process, two types (i.e., pull and push) of loss guidance could be consist to two contact types in our interaction definition. To keep the same data distribution for training and inference, we also use loss guidance in training ControlNet. We can also use loss guidance on x_0 , thus it is no longer needed for training ControlNet, speeding up its training process. In practice, L-BFGS on both x_0 and μ_t could lead to the satisfying alignment of human joints and spatial conditions. We show algorithms of loss guidance on x_0 , μ_t , and interactions in Appendix A.1.

As the root position at frame n is aggregated from all root velocities before frame n in the FK operation, a single condition at frame n is able to affect all previous root positions. It also works for joints other than the root because their global positions are computed from the root position. Thus, our loss guidance could adaptively adjust all previous velocities in frame $[0, n]$ to reach the condition at frame n from a starting point at frame 0. Besides, loss guidance could process any composition of human joints, frames, and XYZ-dim, e.g., controlling left hand and right foot simultaneously at some given frame n .

3.5. Interaction Generation via a LLM-Planner

As loss guidance could optimize a general form of distance measures, we could also optimize losses to avoid obsta-

cles, avoid collisions with others, make people to be face-to-face, or make people’s any joints to be contacted with others. It enables rich interactions with any human joint for an arbitrary number of humans at any time, even it is only trained on single-person data. As we mentioned in Sec 3.1, we define interactions as joint-joint contact pairs. A charming property of our loss guidance in interactions is that both terms in the loss guidance are predicted human joints and could be jointly optimized. Specifically, single-person loss $L(\mu_t, c)$ becomes $L(\mu_t^a, \mu_t^b)$ in interaction scenarios, where a and b are two humans. L-BFGS optimizer will jointly optimize both people by minimizing $L(\mu_t^a, \mu_t^b)$, where μ_t^a and μ_t^b are a and b ’s joints to be contacted.

As we could generate interactions via joint-joint contact pairs, we leverage GPT-4 [39] as the planner to infer text prompts describing multiple people’s action p^{multi} to be single-person prompts p and contact plans \mathcal{C} via prompt engineering. The inputs of the LLM Planner include sentences p^{multi} , background scenario information \mathcal{B} , human joint information \mathcal{J} and pre-set instructions, rules, and examples. Specifically, \mathcal{B} includes number of people, total frames of motion sequence, and video play speed; \mathcal{J} includes all joints’ names (e.g., 22 joints’ names in HumanML3D [13]); rules describe the format of Chain of Contacts and let LLMs to generate plausible contacts and time-steps. Please refer to Appendix A.3 for details of prompts and contact plans.

4. Experiments

Datasets. We conduct experiments on HumanML3D [13] and KIT-ML [43] following MDM [51]. HumanML3D contains 14,646 high-quality human motion sequences from AMASS [38] and HumanAct12 [12], while KIT-ML contains 3,911 motion sequences with more noises.

Evaluation Protocol. We adopt metrics suggested by *Guo et. al.* [13] to evaluate the quality of alignment between text and motion, which are Frechet Inception Distance (**FID**), **R-Precision**, and **Diversity**. We also report metrics related to spatial controls suggested by GMD [25] on HumanML3D dataset, which are **Foot skating ratio**, **Trajectory error**, **Location error** and **Average error**. Please refer to Appendix B.3 or their papers [13, 25] for more details.

Implementation Details. We initialize parameters of both original MDM and Motion ControlNet from pretrained MDM [51] weight and freeze the parameters of original MDM during training. Following MDM [51], we use CLIP [44] model to encode text prompts. We run L-BFGS [35] in loss guidance 5 times for the first 990 denoising steps and 10 times for the last 10 denoising steps on the posterior mean μ_t , and once for the first 990 steps and 10 times for the last 10 steps on clean motion x_0 . We use loss guidance in training ControlNet when using it on μ_t . We set two types of mask $\mathbf{m} \in \{0, 1\}^{N \times J \times 3}$: (1) Only set mask of pelvis (root) joint to 1 for root control to fairly compare with

HumanML3D	FID \downarrow	R-precision \uparrow	Diversity \rightarrow (Top-3)
Real	0.002	0.797	9.503
JL2P [1]	11.02	0.486	7.676
Text2Gesture [3]	7.664	0.345	6.409
T2M [13]	1.067	0.740	9.188
MotionDiffuse [64]	0.630	0.782	9.410
MLD [5]	0.473	0.772	9.724
PhysDiff [61]	0.433	0.631	-
T2M-GPT [62]	0.116	0.775	9.761
MotionGPT [23]	0.232	<u>0.778</u>	<u>9.528</u>
MDM [51]	0.544	0.611	9.446
PriorMDM [47]	0.540	0.640	9.160
GMD [25]	0.212	0.670	9.440
Our InterControl	0.159	0.671	9.482

Table 1. **Text-to-motion evaluation** on HumanML3D [13] dataset. The right arrow \rightarrow means closer to real data is better. Methods in the upper part are unable to perform spatial control.

previous methods; (2) Randomly set one joint to 1 for generally controlling all joints and generate interactions. Each type of mask will be used in both training and inference for consistency. Thus, we get two model weights, where (1) could be fairly compared with previous methods and we use (2) for interaction generation. We use AdamW [37] optimizer and set the learning rate as 1e-5.

4.1. Single-person Motion Generation

Text-conditioned motion generation. To generally compare our InterControl with previous text-conditioned motion generation methods, we report the alignment quality of text and generated motions suggested by *Guo et. al.* [13] in Tab. 1. Note that methods in the upper part of both tables are unable to perform spatial control, thus they are incapable of generating controllable motions and human interactions even if they have lower FID or higher R-precision, e.g., T2M-GPT [62] and MotionGPT [23] tokenize human poses to discrete tokens and is unable to incorporate any spatial information. MLD [5] uses latent diffusion to accelerate denoising steps, yet performing spatial control needs to convert each step of latent feature back to motion representations. It leads to much more computation than MDM [51] and is opposite to MLD’s motivation of using latent diffusion. Among methods that are suitable for spatial control [25, 47] in Tab. 1, our InterControl achieves the best performance in all semantic-level metrics. Due to page limits, please refer to Appendix B.2 for results on KIT-ML.

Spatially controllable motion generation. In Tab. 2, we compare InterControl with other spatially controllable methods [25, 47]. We also include results of MDM [51] to show the controlling metrics [25] without spatial control. The trajectory of MDM could be very different from the desired trajectory without the input control signals, e.g., average error ≥ 1 m. Inpainting-based control is not aware of the

Method	Joint	FID \downarrow	R-precision \uparrow (Top-3)	Diversity \rightarrow	Foot skating ratio \downarrow	Traj. err. \downarrow (50 cm)	Loc. err. \downarrow (50 cm)	Avg. err. \downarrow (m)
Real MDM	No Control	0.002	0.797	9.503	0.0000	0.0000	0.0000	0.0000
		0.544	0.611	9.446	0.0943	0.8909	0.6015	1.1843
PriorMDM †	Root	0.498	0.586	9.167	0.0924	0.3726	0.2210	0.4552
GMD †		0.276	0.655	9.245	0.1108	0.0987	0.0356	0.1457
Ours (root)		0.159	0.671	9.482	0.0729	0.0132	0.0004	0.0496
Ours (all)	Random one	0.178	0.669	9.498	0.0968	0.0403	0.0031	0.0741
Ours (all)	Random two	0.184	0.670	9.410	0.0948	0.0475	0.0030	0.0911
Ours (all)	Random three	0.199	0.673	9.352	0.0930	0.0487	0.0026	0.0969

Table 2. **Spatial control** results on the HumanML3D [13] dataset. *Ours (root)* means model only trained on root control, and *Ours (all)* means model trained on all joints. *Random One/Two/Three* reports the average performance over 1/2/3 randomly selected joints in evaluation. \rightarrow means closer to real data is better. † means our evaluation on their model.

Item	Method	FID \downarrow	R-precision \uparrow (Top-3)	Diversity \rightarrow	Foot skating ratio \downarrow	Traj. err. \downarrow (50 cm)	Loc. err. \downarrow (50 cm)	Avg. err. \downarrow (m)
(1)	Ours (all)	0.178	0.669	9.498	0.0968	0.0403	0.0031	0.0741
(2)	w/o ControlNet	0.965	0.621	9.216	0.1624	0.0879	0.0059	0.1013
(3)	w/ original c	0.227	0.656	9.544	0.1004	0.0697	0.0042	0.0785
(4)	w/o loss guidance	0.187	0.664	9.598	0.0704	0.8569	0.4553	0.6557
(5)	loss guidance on x_0	0.211	0.668	9.394	0.1164	0.0907	0.0088	0.0981
(6)	w/ 1-st order grad	0.198	0.668	9.472	0.0987	0.0879	0.0096	0.0877
(7)	sparsity = 0.25	0.248	0.671	9.442	0.0801	0.0106	0.0007	0.0546
(8)	sparsity = 0.025	0.255	0.663	9.520	0.0705	0.0015	0.0001	0.0067

Table 3. **Ablation studies** on the HumanML3D [13] dataset.

spatial information in the global space, so PriorMDM [47] also has a large divergence with the desired spatial information. The most recent work GMD [25] first generates trajectories in the global space, so it achieves better performance in spatial control metrics. However, it could only control the root joint, limiting its ability in spatial control and interaction generation. Our InterControl could achieve very small errors in spatial control metrics for all-joint control thanks to the power of Inverse Kinematics and L-BFGS optimizer. Meanwhile, Motion ControlNet could ensure the motion data is still in the same distribution with the training set by adapting to the posterior mean updated by loss guidance in its training stage, leading to even better FID than previous methods. It is worth noting that we only use a single model to learn the control strategy for all joints, while previous method [47] needs to train separate models and blend them to inpaint multiple joints. Our method achieves similar performance with controlling one joint when extending it to control multiple joints (last two rows in Tab. 2). We also show results with specific joints in Appendix B.1.

4.2. Ablation Studies

To further investigate the effectiveness of InterControl, we ablate our method in Tab. 3 and reveal some key information in controlling the motion generation model in the global space. Then we also analyze the computational costs of our method to ensure our control is efficient. We will refer to

the variants of InterControl by row numbers in Tab. 3. All experiments are trained on all joints and evaluated with randomly selected joints to report average performance.

Motion ControlNet. By dropping ControlNet, we find that loss guidance could still follow spatial controls with very low errors, yet the motion quality (e.g., FID) is significantly damaged (row 1 vs. row 2). Our ControlNet could adapt to the posterior distribution updated by loss guidance, and produce high-quality motion data. We also find that our c^{final} provides key information in controlling all joints: For root control only, the FID of c^{final} and c shows small difference. However, the FID of root control is always slightly better than all-joint control (~ 0.07) when we use c , indicating insufficient information in all-joint control. We alleviate this by introducing extra information in c^{final} for Motion ControlNet and improve the FID of all-joint control from 0.227 (row 3) to 0.178 (row 1).

Loss Guidance. By dropping loss guidance, our ControlNet itself can produce good semantic-level metrics (e.g., FID) compared with MDM by incorporating extra spatial information (row 4). However, this variant will lead to high spatial errors and cannot strictly follow spatial controls in global space. As the precise joint location is vital for interaction generation, loss guidance is important for our InterControl. Another variant is updating loss guidance on ControlNet’s prediction x_0 (row 5), instead of the posterior mean μ_t . Its advantage is faster training speed because loss

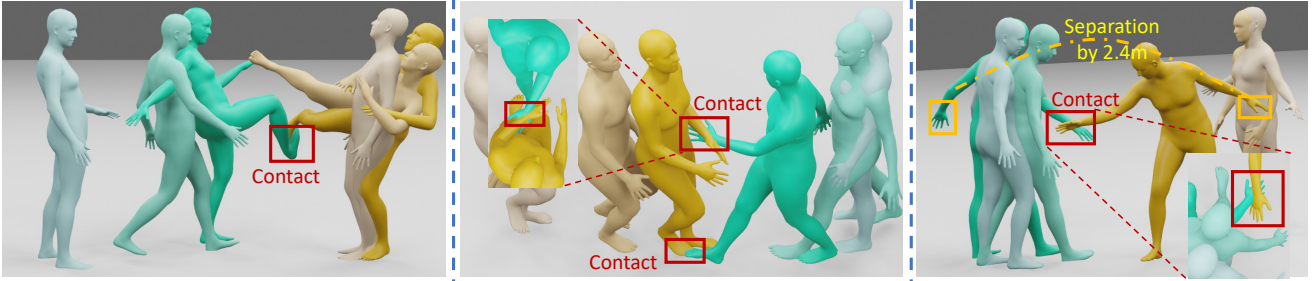


Figure 3. **More visualizations of interactions.** We control interactions by letting any joints contacted or separated by a desired distance.

Sub- Modules	MDM	+ Control Module	+ Guidance $t \in [10, 999]$	+ Guidance $t \in [0, 9]$
Time (s)	39.1	57.3	76.5	80.1

Table 4. **Inference time analysis** on a NVIDIA A100 GPU.

guidance is no longer needed in training ControlNet, which is similar to classifier guidance [8], yet it leads to slightly worse FID than using μ_t . We believe the reason is that loss guidance still changes the data distribution in denoising steps even if it is updated on x_0 . Finally, we also report the result of 1-st order gradient in classifier guidance [8] (row 6) instead of L-BFGS. We find it takes more computations to achieve similar performance with L-BFGS, which is analyzed below.

Inference time analysis. In practice, we find that loss guidance in last few denoising steps (e.g., $t \in [0, 9]$) is vital for precise joint control, while most denoising steps $t \in [10, 999]$ are less important yet take most of computations. Loss guidance on x_0 with only once L-BFGS in $t \in [10, 999]$ and 10 times in $t \in [0, 9]$ could leads FID 0.234 in controlling all joints, yet leads to minimal extra computations. We report its total inference time of 1000 denoising steps by adding sub-modules step-by-step in Tab. 4. GMD [25] needs 110s to run two-stage diffusion models, while we only needs 80s. Gradient-based optimization needs more than 120s to achieve similar control quality. Thanks to GPU’s parallel computing, generating a batch of 32 people in InterControl only needs 91s, enabling efficient group motion generation.

Sparse control signals in temporal. As a key challenge of spatial control is the sparsity, we also report results with sparsely selected frames as control (sparsity = 0.25 and 0.025) in Tab. 3 (row 7 and 8). Our model shows consistent performance of both spatial errors and semantic-level metrics on sparse signals, e.g., FID 0.255 and avg. err. 0.0467 with sparsity 0.025, while GMD [25] achieves FID 0.523 and avg. err. 0.139 with the same sparsity.

4.3. Generate Human Motion Interactions

In Tab. 5, we report spatial-related metrics of InterControl’s zero-shot human interaction generation. Specifically, we collect 100 descriptions of two-person actions from Inter-Human Dataset [34] and let LLM translate them into task

	Traj. err. ↓ (20 cm)	Loc. err. ↓ (20 cm)	Avg. err. ↓ (m)
InterControl	0.0082	0.0005	0.0084

Table 5. **Spatial errors evaluation** on two-person interactions, joint-pairs are collected from task plans generated by LLM.

plans of single-person motion descriptions and joint-joint contact pairs via prompt engineering. Each description will be used to generate 10 different task plans in time and contact joints, thus we collected about 1000 spatial conditions in total from LLMs. Then, we utilize an InterControl model pretrained on the HumanML3D dataset to generate human interactions conditioned on text prompts and joint contact pairs. The spatial-related metrics are reported over controlled joints and frames. InterControl achieves good performance of spatial errors in interaction scenarios, indicating its robustness in precise spatial control. We show visualizations of interactions in Fig. 1 and Fig. 3, where we generate them by controlling the relation of one or two joints of all people. We could make joint pairs be **contacted** or **separated** by distance set by users via loss guidance for generating interactions, e.g., handshaking or kicking off. We let one pair of hands (or feet) be closed while another pair of hands (or feet) be far away by at least a given distance (feet in Fig. 1 and hands in Fig. 3). We could also make all three people’s feet contacted at the same time (Fig. 1) by hand-crafted text prompts and masks, which is infeasible in two-person interaction generation models if they model two people’s interaction as a joint distribution and let diffusion model to learn such joint distribution.

5. Conclusion and Limitations

We presented InterControl, a spatially controllable model diffusion model trained on single-person motion data, that could generate interactive human motions with an arbitrary number of people. We achieve this by enabling a text-conditioned motion generation model with the ability to control every joint of every person at any time. We propose two complementary modules, named Motion ControlNet and Loss Guidance, to improve both the spatial alignment between joints and desired positions, and the overall quality of whole motions. Extensive experiments are conducted on

HumanML3D and KIT-ML benchmarks to validate the effectiveness and efficiency of our proposed modules. Finally, we enable InterControl the ability of text-conditioned interaction generation by leveraging the knowledge of LLMs. Qualitative results validate that InterControl could generate high-quality interactions by precise spatial joint control.

Limitations. As InterControl is not trained on multi-person data, its definition of interaction is based on being *contacted* or *avoided* by some distances for all joints. Motion quality of InterControl is from single-person motion data, and the plausibility of interactions is based on the knowledge of LLMs, i.e., in which degree the joint contact plans are consistent to the semantics of group motion descriptions. Yet, InterControl enables generating interactions of an arbitrary number of humans.

References

- [1] Chaitanya Ahuja and Louis-Philippe Morency. Language2pose: Natural language grounded pose forecasting. In *3DV*. IEEE, 2019. 6
- [2] Tenglong Ao, Qingzhe Gao, Yuke Lou, Baoquan Chen, and Libin Liu. Rhythmic gesticulator: Rhythm-aware co-speech gesture synthesis with hierarchical neural embeddings. *ACM Trans. Graph.*, 2022. 2, 3
- [3] Uttaran Bhattacharya, Nicholas Rewkowski, Abhishek Banerjee, Pooja Guhan, Aniket Bera, and Dinesh Manocha. Text2gestures: A transformer-based network for generating emotive body gestures for virtual agents. In *VR*. IEEE, 2021. 6
- [4] Tom B. Brown, Benjamin Mann, Nick Ryder, Melanie Subbiah, Jared Kaplan, Prafulla Dhariwal, Arvind Neelakantan, Pranav Shyam, Girish Sastry, Amanda Askell, Sandhini Agarwal, Ariel Herbert-Voss, Gretchen Krueger, Tom Henighan, Rewon Child, Aditya Ramesh, Daniel M. Ziegler, Jeffrey Wu, Clemens Winter, Christopher Hesse, Mark Chen, Eric Sigler, Mateusz Litwin, Scott Gray, Benjamin Chess, Jack Clark, Christopher Berner, Sam McCandlish, Alec Radford, Ilya Sutskever, and Dario Amodei. Language models are few-shot learners. In *NeurIPS*, 2020. 2
- [5] Xin Chen, Biao Jiang, Wen Liu, Zilong Huang, Bin Fu, Tao Chen, and Gang Yu. Executing your commands via motion diffusion in latent space. In *CVPR*, 2023. 2, 3, 4, 6, 13
- [6] Jooyoung Choi, Sungwon Kim, Yonghyun Jeong, Youngjune Gwon, and Sungroh Yoon. ILVR: conditioning method for denoising diffusion probabilistic models. In *ICCV*, 2021. 3
- [7] Hyungjin Chung, Byeongsu Sim, Dohoон Ryu, and Jong Chul Ye. Improving diffusion models for inverse problems using manifold constraints. In *NeurIPS*, 2022. 3
- [8] Prafulla Dhariwal and Alexander Quinn Nichol. Diffusion models beat gans on image synthesis. In *NeurIPS*, 2021. 2, 3, 4, 5, 8
- [9] Yinglin Duan, Tianyang Shi, Zhengxia Zou, Yenan Lin, Zhehui Qian, Bohan Zhang, and Yi Yuan. Single-shot motion completion with transformer. *arXiv preprint arXiv:2103.00776*, 2021. 2, 3
- [10] Patrick Esser, Johnathan Chiu, Parmida Atighehchian, Jonathan Granskog, and Anastasis Germanidis. Structure and content-guided video synthesis with diffusion models. In *ICCV*, 2023. 3
- [11] Anindita Ghosh, Rishabh Dabral, Vladislav Golyanik, Christian Theobalt, and Philipp Slusallek. Imos: Intent-driven full-body motion synthesis for human-object interactions. *Comput. Graph. Forum*, 2023. 3
- [12] Chuan Guo, Xinxin Zuo, Sen Wang, Shihao Zou, Qingyao Sun, Annan Deng, Minglun Gong, and Li Cheng. Action2motion: Conditioned generation of 3d human motions. In *ACM MM*, 2020. 2, 3, 6
- [13] Chuan Guo, Shihao Zou, Xinxin Zuo, Sen Wang, Wei Ji, Xingyu Li, and Li Cheng. Generating diverse and natural 3d human motions from text. In *CVPR*, 2022. 1, 2, 3, 4, 6, 7, 12, 13
- [14] Chuan Guo, Xinxin Zuo, Sen Wang, and Li Cheng. Tm2t: Stochastic and tokenized modeling for the reciprocal generation of 3d human motions and texts. In *ECCV*, 2022. 2, 3
- [15] Yuwei Guo, Ceyuan Yang, Anyi Rao, Yaohui Wang, Yu Qiao, Dahua Lin, and Bo Dai. Animatediff: Animate your personalized text-to-image diffusion models without specific tuning. *arXiv preprint arXiv:2307.04725*, 2023. 3
- [16] Ikhsanul Habibie, Mohamed Elgharib, Kripasindhu Sarkar, Ahsan Abdullah, Simbarashe Nyatsanga, Michael Neff, and Christian Theobalt. A motion matching-based framework for controllable gesture synthesis from speech. In *SIGGRAPH (Conference Paper Track)*, 2022. 2, 3
- [17] Félix G Harvey, Mike Yurick, Derek Nowrouzezahrai, and Christopher Pal. Robust motion in-betweening. *ACM Transactions on Graphics (TOG)*, 2020. 2, 3
- [18] Mohamed Hassan, Duygu Ceylan, Ruben Villegas, Jun Saito, Jimei Yang, Yi Zhou, and Michael J. Black. Stochastic scene-aware motion prediction. In *ICCV*, 2021. 3
- [19] Kaiming He, Xiangyu Zhang, Shaoqing Ren, and Jian Sun. Deep residual learning for image recognition. In *CVPR*, 2016. 12
- [20] Jonathan Ho and Tim Salimans. Classifier-free diffusion guidance. *arXiv preprint arXiv:2207.12598*, 2022. 3, 4
- [21] Jonathan Ho, Ajay Jain, and Pieter Abbeel. Denoising diffusion probabilistic models. In *NeurIPS*, 2020. 1
- [22] Jonathan Ho, William Chan, Chitwan Saharia, Jay Whang, Ruiqi Gao, Alexey Gritsenko, Diederik P Kingma, Ben Poole, Mohammad Norouzi, David J Fleet, et al. Imagen video: High definition video generation with diffusion models. *arXiv preprint arXiv:2210.02303*, 2022. 3
- [23] Biao Jiang, Xin Chen, Wen Liu, Jingyi Yu, Gang Yu, and Tao Chen. Motiongpt: Human motion as a foreign language. *arXiv preprint arXiv:2306.14795*, 2023. 6, 13
- [24] Nan Jiang, Tengyu Liu, Zhexuan Cao, Jieming Cui, Yixin Chen, He Wang, Yixin Zhu, and Siyuan Huang. Chairs: Towards full-body articulated human-object interaction. *arXiv preprint arXiv:2212.10621*, 2022. 3
- [25] Korrawe Karunratanakul, Konpat Preechakul, Supasorn Suwajanakorn, and Siyu Tang. Guided motion diffusion for controllable human motion synthesis. In *CVPR*, 2023. 2, 3, 4, 6, 7, 8, 12, 13

[26] Manuel Kaufmann, Emre Aksan, Jie Song, Fabrizio Pece, Remo Ziegler, and Otmar Hilliges. Convolutional auto-encoders for human motion infilling. In *3DV*, 2020. 3

[27] Jongmin Kim, Yeongho Seol, and Taesoo Kwon. Interactive multi-character motion retargeting. *Comput. Animat. Virtual Worlds*, 2021. 3

[28] Jihoon Kim, Jiseob Kim, and Sungjoon Choi. FLAME: free-form language-based motion synthesis & editing. In *AAAI*, 2023. 3

[29] Diederik P. Kingma and Max Welling. Auto-encoding variational bayes. In *ICLR*, 2014. 1, 3

[30] Zhifeng Kong, Wei Ping, Jiaji Huang, Kexin Zhao, and Bryan Catanzaro. Diffwave: A versatile diffusion model for audio synthesis. *arXiv preprint arXiv:2009.09761*, 2020. 3

[31] Nilesh Kulkarni, Davis Rempe, Kyle Genova, Abhijit Kundu, Justin Johnson, David Fouhey, and Leonidas Guibas. Nifty: Neural object interaction fields for guided human motion synthesis. *arXiv preprint arXiv:2307.07511*, 2023. 3

[32] Buyu Li, Yongchi Zhao, Shi Zhelun, and Lu Sheng. Danceformer: Music conditioned 3d dance generation with parametric motion transformer. In *AAAI*, 2022. 2, 3

[33] Ruilong Li, Shan Yang, David A Ross, and Angjoo Kanazawa. Ai choreographer: Music conditioned 3d dance generation with aist++. In *ICCV*, 2021. 2, 3

[34] Han Liang, Wenqian Zhang, Wenxuan Li, Jingyi Yu, and Lan Xu. Intergen: Diffusion-based multi-human motion generation under complex interactions. *arXiv preprint arXiv:2304.05684*, 2023. 8, 12

[35] Dong C. Liu and Jorge Nocedal. On the limited memory BFGS method for large scale optimization. *Math. Program.*, 1989. 2, 5, 6, 11

[36] Matthew Loper, Naureen Mahmood, Javier Romero, Gerard Pons-Moll, and Michael J. Black. SMPL: a skinned multi-person linear model. *ACM Trans. Graph.*, 2015. 4

[37] Ilya Loshchilov and Frank Hutter. Decoupled weight decay regularization. In *ICLR (Poster)*, 2019. 6

[38] Naureen Mahmood, Nima Ghorbani, Nikolaus F Troje, Gerard Pons-Moll, and Michael J Black. Amass: Archive of motion capture as surface shapes. In *ICCV*, 2019. 6

[39] OpenAI. GPT-4 technical report. *arXiv preprint arXiv:2303.08774*, 2023. 6, 12

[40] Georgios Pavlakos, Vasileios Choutas, Nima Ghorbani, Timo Bolkart, Ahmed A. A. Osman, Dimitrios Tzionas, and Michael J. Black. Expressive body capture: 3d hands, face, and body from a single image. In *CVPR*, 2019. 2

[41] Mathis Petrovich, Michael J Black, and GÜl Varol. Action-conditioned 3d human motion synthesis with transformer vae. In *ICCV*, 2021. 2, 3

[42] Mathis Petrovich, Michael J Black, and GÜl Varol. Temos: Generating diverse human motions from textual descriptions. In *ECCV*, 2022. 2, 3

[43] Matthias Plappert, Christian Mandery, and Tamim Asfour. The KIT motion-language dataset. *Big Data*, 2016. 2, 6, 13

[44] Alec Radford, Jong Wook Kim, Chris Hallacy, Aditya Ramesh, Gabriel Goh, Sandhini Agarwal, Girish Sastry, Amanda Askell, Pamela Mishkin, Jack Clark, Gretchen Krueger, and Ilya Sutskever. Learning transferable visual models from natural language supervision. In *ICML*, 2021. 6

[45] Davis Rempe, Zhengyi Luo, Xue Bin Peng, Ye Yuan, Kris Kitani, Karsten Kreis, Sanja Fidler, and Or Litany. Trace and pace: Controllable pedestrian animation via guided trajectory diffusion. In *CVPR*, 2023. 3

[46] Robin Rombach, Andreas Blattmann, Dominik Lorenz, Patrick Esser, and Björn Ommer. High-resolution image synthesis with latent diffusion models. In *CVPR*, 2022. 3, 4

[47] Yonatan Shafir, Guy Tevet, Roy Kapon, and Amit H Bermano. Human motion diffusion as a generative prior. *arXiv preprint arXiv:2303.01418*, 2023. 2, 3, 4, 6, 7, 12, 13

[48] Jiaming Song, Qinsheng Zhang, Hongxu Yin, Morteza Mardani, Ming-Yu Liu, Jan Kautz, Yongxin Chen, and Arash Vahdat. Loss-guided diffusion models for plug-and-play controllable generation. In *ICML*, 2023. 5

[49] Yang Song, Jascha Sohl-Dickstein, Diederik P. Kingma, Abhishek Kumar, Stefano Ermon, and Ben Poole. Score-based generative modeling through stochastic differential equations. In *ICLR*, 2021. 1, 3, 4

[50] Sebastian Starke, He Zhang, Taku Komura, and Jun Saito. Neural state machine for character-scene interactions. *ACM Trans. Graph.*, 2019. 3

[51] Guy Tevet, Sigal Raab, Brian Gordon, Yonatan Shafir, Daniel Cohen-Or, and Amit Haim Bermano. Human motion diffusion model. In *ICLR*, 2023. 2, 3, 4, 6, 13

[52] Jonathan Tseng, Rodrigo Castellon, and C. Karen Liu. EDGE: editable dance generation from music. In *CVPR*, 2023. 2, 3

[53] Joris Vaillant, Karim Bouyarmane, and Abderrahmane Kheddar. Multi-character physical and behavioral interactions controller. *IEEE Trans. Vis. Comput. Graph.*, 2017. 3

[54] Ashish Vaswani, Noam Shazeer, Niki Parmar, Jakob Uszkoreit, Llion Jones, Aidan N. Gomez, Łukasz Kaiser, and Illia Polosukhin. Attention is all you need. In *NIPS*, 2017. 3, 4

[55] Jiashun Wang, Huazhe Xu, Jingwei Xu, Sifei Liu, and Xiaolong Wang. Synthesizing long-term 3d human motion and interaction in 3d scenes. In *CVPR*, 2021. 3

[56] Jingbo Wang, Sijie Yan, Bo Dai, and Dahua Lin. Scene-aware generative network for human motion synthesis. In *CVPR*, 2021.

[57] Zan Wang, Yixin Chen, Tengyu Liu, Yixin Zhu, Wei Liang, and Siyuan Huang. HUMANISE: language-conditioned human motion generation in 3d scenes. In *NeurIPS*, 2022.

[58] Zeqi Xiao, Tai Wang, Jingbo Wang, Jinkun Cao, Wenwei Zhang, Bo Dai, Dahua Lin, and Jiangmiao Pang. Unified human-scene interaction via prompted chain-of-contacts. *arXiv preprint arXiv:2309.07918*, 2023. 2, 3

[59] Yiming Xie, Varun Jampani, Lei Zhong, Deqing Sun, and Huaiyu Jiang. Omnicontrol: Control any joint at any time for human motion generation. *arXiv preprint arXiv:2310.08580*, 2023. 3, 12

[60] Sirui Xu, Zhengyuan Li, Yu-Xiong Wang, and Liang-Yan Gui. Interdiff: Generating 3d human-object interactions with physics-informed diffusion. In *ICCV*, 2023. 3

Algorithm 1 Single-person model inference with \mathbf{x}_0

Require: a Motion Diffusion Model M with parameter θ , a Motion ControlNet C with parameter ϕ , original spatial condition \mathbf{c} and spatial condition with extra information \mathbf{c}^{final} , text prompts \mathbf{p} , number of L-BFGS K .

- 1: $\mathbf{x}_T \sim \mathcal{N}(0, \mathbf{I})$
- 2: **for** t from T to 1 **do**
- 3: # Motion ControlNet
- 4: $\{\mathbf{f}\} \leftarrow C(\mathbf{x}_t, t, \mathbf{p}, \mathbf{c}^{final}; \phi)$
- 5: # Motion Diffusion Model
- 6: $\mathbf{x}_0 \leftarrow M(\mathbf{x}_t, t, \mathbf{p}, \{\mathbf{f}\}; \theta)$
- 7: **for** k from 1 to K **do**
- 8: $\mathbf{x}_0 \leftarrow \text{L-BFGS}(L(\mathbf{x}_0, \mathbf{c}))$ # Loss Guidance
- 9: **end for**
- 10: $\mu_t, \Sigma_t \leftarrow \mu(\mathbf{x}_0, \mathbf{x}_t), \Sigma_t$ # Posterior
- 11: $\mathbf{x}_{t-1} \sim \mathcal{N}(\mu_t, \Sigma_t)$
- 12: **end for**
- 13: **return** \mathbf{x}_0

- [61] Ye Yuan, Jiaming Song, Umar Iqbal, Arash Vahdat, and Jan Kautz. Physdiff: Physics-guided human motion diffusion model. In *ICCV*, 2023. 3, 4, 6
- [62] Jianrong Zhang, Yangsong Zhang, Xiaodong Cun, Yong Zhang, Hongwei Zhao, Hongtao Lu, Xi Shen, and Shan Ying. Generating human motion from textual descriptions with discrete representations. In *CVPR*, 2023. 6, 13
- [63] Lvmi Zhang, Anyi Rao, and Maneesh Agrawala. Adding conditional control to text-to-image diffusion models. In *ICCV*, 2023. 2, 3, 4, 5
- [64] Mingyuan Zhang, Zhongang Cai, Liang Pan, Fangzhou Hong, Xinying Guo, Lei Yang, and Ziwei Liu. Motiondiffuse: Text-driven human motion generation with diffusion model. *arXiv preprint arXiv:2208.15001*, 2022. 2, 3, 6, 13
- [65] Yunbo Zhang, Deepak Gopinath, Yuting Ye, Jessica K. Hodgins, Greg Turk, and Jungdam Won. Simulation and retargeting of complex multi-character interactions. In *SIGGRAPH (Conference Paper Track)*, 2023. 3
- [66] Kaifeng Zhao, Yan Zhang, Shaofei Wang, Thabo Beeler, and Siyu Tang. Synthesizing diverse human motions in 3d indoor scenes. *arXiv preprint arXiv:2305.12411*, 2023. 3

A. More Details about InterControl

A.1. Pseudo-code of Loss Guidance

Here we elaborate the details of Loss Guidance's algorithm. As we mentioned in the main paper, Loss guidance could be performed on predicted clean motion (i.e., \mathbf{x}_0) or posterior mean in denoising step t (i.e., μ_t). In practice, we find that \mathbf{x}_0 works well in root control, and it does not require loss guidance in training Motion ControlNet, leading to faster training speed. Besides, it also requires less times of L-BFGS [35], which means faster inference speed. μ_t leads to better FID in controlling all joints, yet it requires more

Algorithm 2 Single-person model inference with μ_t

Require: a Motion Diffusion Model M with parameter θ , a Motion ControlNet C with parameter ϕ , original spatial condition \mathbf{c} and spatial condition with extra information \mathbf{c}^{final} , text prompts \mathbf{p} , number of L-BFGS K .

- 1: $\mathbf{x}_T \sim \mathcal{N}(0, \mathbf{I})$
- 2: **for** t from T to 1 **do**
- 3: # Motion ControlNet
- 4: $\{\mathbf{f}\} \leftarrow C(\mathbf{x}_t, t, \mathbf{p}, \mathbf{c}^{final}; \phi)$
- 5: # Motion Diffusion Model
- 6: $\mathbf{x}_0 \leftarrow M(\mathbf{x}_t, t, \mathbf{p}, \{\mathbf{f}\}; \theta)$
- 7: $\mu_t, \Sigma_t \leftarrow \mu(\mathbf{x}_0, \mathbf{x}_t), \Sigma_t$ # Posterior
- 8: **for** k from 1 to K **do**
- 9: $\mu_t \leftarrow \text{L-BFGS}(L(\mu_t, \mathbf{c}))$ # Loss Guidance
- 10: **end for**
- 11: $\mathbf{x}_{t-1} \sim \mathcal{N}(\mu_t, \Sigma_t)$
- 12: **end for**
- 13: **return** \mathbf{x}_0

Algorithm 3 Two-people interaction model inference

Require: a Motion Diffusion Model M with parameter θ , a Motion ControlNet C with parameter ϕ , interaction prompts \mathbf{p}^{multi} , number of L-BFGS K , Forward Kinematics operation FK, masked selection operation S .

- 1: $\mathbf{x}_T^a, \mathbf{x}_T^b \sim \mathcal{N}(0, \mathbf{I})$
- 2: **for** t from T to 1 **do**
- 3: # LLM-Planner
- 4: $\mathbf{p}^a, \mathbf{p}^b, \text{mask} \leftarrow \text{LLM}(\mathbf{p}^{multi})$
- 5: # Copy Spatial Condition from Each Other
- 6: $\mathbf{c}^a \leftarrow S(\text{FK}(\mathbf{x}_t^b), \text{mask})$
- 7: $\mathbf{c}^b \leftarrow S(\text{FK}(\mathbf{x}_t^a), \text{mask})$
- 8: # Motion ControlNet
- 9: $\{\mathbf{f}\}^a \leftarrow C(\mathbf{x}_t^a, t, \mathbf{p}^a, \mathbf{c}^a; \phi)$
- 10: $\{\mathbf{f}\}^b \leftarrow C(\mathbf{x}_t^b, t, \mathbf{p}^b, \mathbf{c}^b; \phi)$
- 11: # Motion Diffusion Model
- 12: $\mathbf{x}_0^a \leftarrow M(\mathbf{x}_t^a, t, \mathbf{p}^a, \{\mathbf{f}\}^a; \theta)$
- 13: $\mathbf{x}_0^b \leftarrow M(\mathbf{x}_t^b, t, \mathbf{p}^b, \{\mathbf{f}\}^b; \theta)$
- 14: $\mu_t^a, \Sigma_t \leftarrow \mu(\mathbf{x}_0^a, \mathbf{x}_t^a), \Sigma_t$ # Posterior
- 15: $\mu_t^b, \Sigma_t \leftarrow \mu(\mathbf{x}_0^b, \mathbf{x}_t^b), \Sigma_t$ # Posterior
- 16: **for** k from 1 to K **do**
- 17: # Loss Guidance
- 18: $\mu_t^a, \mu_t^b \leftarrow \text{L-BFGS}(L(\mu_t^a, \mu_t^b))$
- 19: **end for**
- 20: $\mathbf{x}_{t-1}^a \sim \mathcal{N}(\mu_t^a, \Sigma_t)$
- 21: $\mathbf{x}_{t-1}^b \sim \mathcal{N}(\mu_t^b, \Sigma_t)$
- 22: **end for**
- 23: **return** $\mathbf{x}_0^a, \mathbf{x}_0^b$

times of L-BFGS [35] and also need loss guidance in training Motion ControlNet. We show the pseudo-code of InterControl with Loss Guidance on \mathbf{x}_0 in Algorithm 1, and Loss

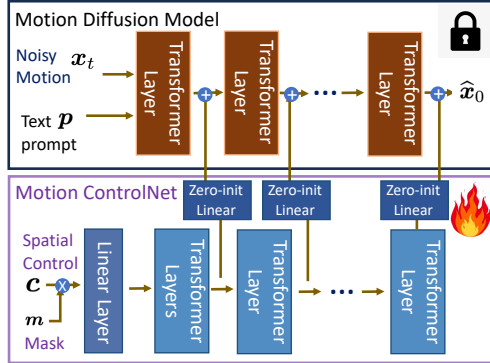


Figure 4. Architecture of Motion ControlNet.

Guidance on μ_t in Algorithm 2. We show the pseudo-code of InterControl in interaction generation in Algorithm 3.

A.2. Details of Motion ControlNet

In this subsection, we elaborate the details of Motion ControlNet’s architecture. Motion ControlNet is designed to adaptively generate realistic and high-fidelity motion sequences based on condition c . It is a trainable copy of MDM, and each transformer encoder layer of ControlNet and the original MDM is connected by a zero-initialized linear layer, as shown in Fig. 4. The parameters in the original MDM is pretrained and frozen in the entire training process. Thus, our framework in the finetuning process starts from the weights that is equivalent to a pretrained MDM due to the zero-initialized linear layers. ControlNet will learn a residual feature for spatial control signals c in each transformer layer by the back-propagated gradients. Thus, our model is able to implicitly adjust model weights for all joints and frames based on a sparse spatial condition c by learning the spatial-level conditional distribution in addition to the semantic-level distribution.

To process condition c , the uncontrolled joints, frames and XYZ-dim are masked as 0. Then we use a linear layer to project the condition $c \in \mathbb{R}^{N \times 3J}$ to the hidden dimension of transformer layers as $c^H \in \mathbb{R}^{N \times D^H}$, and feed c' to transformer encoder layers in ControlNet. We use a zero-initialized linear layer to link the output of each layer in ControlNet to the transformer encoder layer of pretrained and frozen MDM via a residual connection [19]. We use extra information as condition for Motion ControlNet $c^{final} = cat(c', c'', n^s, n^h)$. The details of c^{final} has been explained in Sec 3.3 in our main paper.

A.3. LLM-Planner

In this section, we further elaborate the details of LLM Planner. Specifically, we collect 100 sentences describing human interactions with joint contacts from the description of InterHuman Dataset [34]. Then, we use a GPT-4 [39] with the prompt in Tab. 8 to let GPT-4 to produce joint-joint contact plans for us. For each collected sentence, we replace

it as the *instruction* in the prompt, and LLM will generate 10 task plans for us, as shown in Tab. 9. We manually correct typos of task plans generated by LLM, such as typos of joint name, invalid joint name, or invalid start frame or end frame. It leads to 989 valid task plans. Finally, we write Python scripts to transform the natural language tasks plans to Python Json format, as shown in Tab. 10. We take single-person language prompts in task plans as texts for motion diffusion model, and transform information in ‘steps’ to joint contact masks in the spatial condition. Specifically, we update the other person’s joint positions as the current person’s spatial condition in each denoising step, and use the spatial condition to guide Motion ControlNet and Loss Guidance in the same way with single-person scenarios. We evaluate the quality of interactions by using metrics like trajectory error and average error proposed by GMD [25] in the same way with single-person scenarios. We only evaluate on joints and frames in the joint-joint contact pairs. The result on our collected 989 task plans is shown in Tab. 5 in the main paper.

B. Additional Experiments

B.1. More Single-joint Control Results

In Tab. 2 of our main paper, we have shown the spatial control results with root joint and randomly selected one/two/three joints. Following the concurrent work [59], we also show the spatial control performance on specific joints in Tab. 6. We find that feet and hands are more difficult to control due to their flexibility, while root (pelvis) and head are more easier to follow, leading to better FID and R-precision.

B.2. Compare with Previous Methods in KIT-ML

Due to the noisy motion data in KIT-ML, incorporating spatial information has no contribution to these metrics. Instead, the noisy spatial information may lead to implausible human poses and further degrade the performance of controllable methods, e.g., PriorMDM [47] is an inpainting version of MDM and has worse FID. Our InterControl is better than other controllable methods on KIT-ML.

B.3. Details of Evaluation Metrics

Here we select some descriptions for metrics used to evaluate controllable motion generation methods from HumanML3D [13] and GMD [25] to save reader’s time.

Semantic-level Evaluation Metrics from HumanML3D [13]: Frechet Inception Distance (FID), diversity and multi-modality. For quantitative evaluation, a motion feature extractor and text feature extractor is trained under contrastive loss to produce geometrically close feature vectors for matched text-motion pairs, and vice versa. Further explanations of aforementioned metrics

Method	Joint	FID \downarrow	R-precision \uparrow (Top-3)	Diversity \rightarrow	Foot skating ratio \downarrow	Traj. err. \downarrow (50 cm)	Loc. err. \downarrow (50 cm)	Avg. err. \downarrow (m)
Ours (all)	Root	0.184	0.672	9.315	0.1044	0.0317	0.0018	0.0693
Ours (all)	Left foot	0.242	0.664	9.184	0.1005	0.0696	0.0024	0.0671
Ours (all)	Right foot	0.236	0.669	9.201	0.0983	0.0798	0.0029	0.0680
Ours (all)	Head	0.172	0.678	9.359	0.0958	0.0523	0.0044	0.0846
Ours (all)	Left wrist	0.260	0.660	8.965	0.0915	0.0375	0.0012	0.0874
Ours (all)	Right wrist	0.284	0.655	9.003	0.0920	0.0364	0.0010	0.0872

Table 6. **Spatial control** results on the HumanML3D [13] dataset. *Ours (all)* means the model is trained on one randomly selected joint among all joints in each iteration.

KIT-ML	FID \downarrow	R-precision \uparrow (Top-3)	Diversity \rightarrow
Real	0.031	0.779	11.08
T2M [13]	3.022	0.681	10.72
MotionDiffuse [64]	1.954	<u>0.739</u>	11.10
MLD [5]	0.404	0.734	10.80
T2M-GPT [62]	0.514	0.745	<u>10.92</u>
MotionGPT [23]	0.510	0.680	10.35
MDM [51]	<u>0.497</u>	0.396	10.84
PriorMDM [†] [47]	0.830	0.397	10.54
GMD [†] [25]	1.537	0.385	9.78
Our InterControl	0.580	0.397	10.88

Table 7. **Text-to-motion evaluation** on the KIT-ML [43] dataset. Methods in the upper part are unable to perform spatial control. [†] means our implementation, they do not report results on KIT-ML.

as well as the specific textual and motion feature extractor are relegated to the supplementary file due to space limit. In addition, the R-precision and MultiModal distance are proposed in this work as complementary metrics, as follows. Consider R-precision: for each generated motion, its ground-truth text description and 31 randomly selected mismatched descriptions from the test set form a description pool. This is followed by calculating and ranking the Euclidean distances between the motion feature and the text feature of each description in the pool. We then count the average accuracy at top-1, top-2 and top-3 places. The ground truth entry falling into the top-k candidates is treated as successful retrieval, otherwise it fails. Meanwhile, MultiModal distance is computed as the average Euclidean distance between the motion feature of each generated motion and the text feature of its corresponding description in test set.

Spatial-level Evaluation Metrics from GMD [25]: We use Trajectory diversity, Trajectory error, Location error, and Average error of keyframe locations. Trajectory diversity measures the root mean square distance of each location of each motion step from the average location of that motion step across multiple samples with the same settings. Trajectory error is the ratio of unsuccessful trajectories, de-

fined as those with any keyframe location error exceeding a threshold. Location error is the ratio of keyframe locations that are not reached within a threshold distance. Average error measures the mean distance between the generated motion locations and the keyframe locations measured at the keyframe motion steps.

Table 8. **Detailed prompting example of the LLM Planner.**

Input
Instruction: two people greet each other with a handshake, while holding their cards in the left hand.
Given the instruction, generate 10 task plans according to the following background information, rules, and examples. Each task plan should completely reflect an entire process of actions described in the instruction.
[start of background Information]
Human has JOINTS: ['pelvis', 'left_hip', 'right_hip', 'left_knee', 'right_knee', 'left_ankle', 'right_ankle', 'left_foot', 'right_foot', 'neck', 'left_collar', 'right_collar', 'head', 'left_shoulder', 'right_shoulder', 'left_elbow', 'right_elbow', 'left_wrist', 'right_wrist'].
The total number of TIME-STEPs of human motion is 99, the frame-per-second of motion is 20.
The provided text instruction is describing two people performing some actions containing human joint contacts.
The height of all people is 1.8 meters, the arm length is 0.6 meters, and the leg length is 0.9 meters.
Two people are 2 meters away at the beginning (i.e., TIME-STEPs=0).
[end of background Information]
[start of rules]
1. Each task plan should be composite into detailed steps.
2. Each step should contain meaningful joint-joint pairs.
3. Each joint-joint pair should be formatted into {JOINT, JOINT, TIME-STEP, TIME-STEP, CONTACT TYPE, DISTANCE}. JOINT should be replaced by JOINT in the background information. IMPORTANT: The first JOINT belongs to person 1, and the second JOINT belongs to person 2. Each joint-joint pair represents a contact of a joint of person 1 and a joint of person 2. The first TIME-STEP is the start frame number of contact, and the second TIME-STEP is the end frame number of contact. CONTACT TYPE should be selected from {contact, avoid}, DISTANCE should be a float number representing how many meters should be the distance of two joints in the joint-joint pair. For [CONTACT TYPE: contact], the distance of two joints should be SMALLER than the DISTANCE; for [CONTACT TYPE: avoid], the distance of two joints should be LARGER than the DISTANCE. IMPORTANT: Consider the transition of contact types, leave time-steps more than 20 frames without any joint-joint pair between different contact types. Use small DISTANCE variance between different contact types: for the joint-joint pairs that are with [CONTACT TYPE: contact], do NOT use DISTANCE larger than 0.5m in the following [CONTACT TYPE: avoid]; for the joint-joint pairs that are with [CONTACT TYPE: contact], use [CONTACT TYPE: avoid] after 20 frames; for the joint-joint pairs that are with [CONTACT TYPE: avoid], use NO joint pairs for 20 frames if the following CONTACT TYPE is contact. Try to not over-use [CONTACT TYPE: avoid]: if there is no explicit semantics of being far away, just do not use joint-joint pair in that frames; if there is explicit semantics of being far away, then use joint-joint pair with [CONTACT TYPE: avoid].
4. Consider which JOINT will be interacted when two people perform the action described in the text instruction. Translate the text instruction to be steps of joint-joint pairs. Do not include extra joint-joint pairs that is unrelated to the text instruction. IMPORTANT: make joint-joint pairs in different task plans diverse in TIME-STEPs and JOINTs. Each joint-joint contact pairs should be lasting from 3 to 10 frames.
5. Be plausible. Do not generate uncommon interactions. Generate plausible interaction time-steps, and consider the velocity of human motions.
6. Use one sentence to describe what action should person 1 do and one sentence to describe what action should person 2 do according to the text instruction at the beginning of the task plan. IMPORTANT: the sentence starts from 'text 1:' describing the action of person 1 from the perspective of person 1 and the sentence starts from 'text 2:' describing the action of person 2 from the perspective of person 2. Sentences should NOT contain words like 'person 1' or 'person 2', use 'a person' to refer to himself in the sentence and 'others' to refer to others.
7. The steps in the task plan are for both two people. Use one set of steps to describe both two people. The first JOINT belongs to person 1, and the second JOINT belongs to person 2.
8. IMPORTANT: Do NOT add explanations for the steps in task plans. Each step only have one joint-joint pairs.
[end of rules]
[start of an example]
Instruction: two people greet each other with a handshake, while holding their cards in the left hand.
[Start of Plan 1]
Text 1: a person make a handshake with others using his right wrist, while holding his cards in the left wrist.
Text 2: a person make a handshake with others using his right wrist, while holding his cards in the left wrist.
Step 1: {right wrist, right wrist, 0, 10, avoid, 0.3}
Step 2: {right wrist, right wrist, 50, 60, contact, 0.05}
Step 3: {right wrist, right wrist, 90, 100, avoid, 0.3}
[End of Plan 1]
[end of an example]

Table 9. Example of the LLM generated task plans.

LLM Generated Task Plans (only show 5 due to page limit)
Instructions: The first fencer lunges at the second, who parries the attack and counters with a successful strike to the head.
[Start of Plan 1]
Text 1: A person lunges towards another with his right foot.
Text 2: A person parries the lunged attack while preparing to counter.
Step 1: {right_foot, left_knee, 5, 10, contact, 0.3}
Step 2: {right_wrists, left_collar, 20, 30, avoid, 0.3}
Step 3: {left_elbow, head, 70, 80, contact, 0.05}
[End of Plan 1]
[Start of Plan 2]
Text 1: A person lunges at the other person with his right foot.
Text 2: A person blocks the lunged attack.
Step 1: {right_foot, left_ankle, 3, 10, contact, 0.2}
Step 2: {right_wrists, right_collar, 20, 30, avoid, 0.25}
Step 3: {left_wrists, head, 70, 79, contact, 0.02}
[End of Plan 2]
[Start of Plan 3]
Text 1: A person takes a lunge step towards another.
Text 2: A person parries the attack and counters.
Step 1: {right_foot, right_knee, 7, 14, contact, 0.3}
Step 2: {left_wrists, right_collar, 22, 30, avoid, 0.25}
Step 3: {right_wrists, head, 69, 77, contact, 0.03}
[End of Plan 3]
[Start of Plan 4]
Text 1: A person lunges northerly towards another with his left foot.
Text 2: A person parries the attack and prepares a counterattack.
Step 1: {left_foot, right_ankle, 6, 10, contact, 0.35}
Step 2: {left_wrists, left_collar, 22, 30, avoid, 0.28}
Step 3: {right_elbow, head, 71, 80, contact, 0.05}
[End of Plan 4]
[Start of Plan 5]
Text 1: A person lunges at another using his right foot.
Text 2: A person deflects the approaching lunge and immediately counters.
Step 1: {right_foot, left_knee, 4, 12, contact, 0.31}
Step 2: {left_wrists, right_shoulder, 20, 30, avoid, 0.3}
Step 3: {right_wrists, head, 73, 81, contact, 0.05}
[End of Plan 5]

Table 10. Example of processed json file from task plans generated by LLM.

Processed Json format, (only show 3 due to page limit)
Format of 'steps': [[index of contact joint of person 1, index of contact joint of person 2, start frame, end frame, contact type (contact = 1, avoidance = 0), desired distance (unit as meter)], ...,].
[
{
"text_person1": "A person lunges towards another with his right foot.",
"text_person2": "A person parries the lunged attack while preparing to counter.",
"steps": [
[11, 4, 5, 10, 1, 0.3],
[21, 13, 30, 40, 0, 0.3],
[18, 15, 70, 80, 1, 0.05]
]
},
{
"text_person1": "A person lunges at the other person with his right foot.",
"text_person2": "A person blocks the lunged attack.",
"steps": [
[11, 7, 3, 10, 1, 0.2],
[21, 14, 30, 40, 0, 0.25],
[20, 15, 70, 79, 1, 0.02]
]
},
{
"text_person1": "A person takes a lunge step towards another.",
"text_person2": "A person parries the attack and counters.",
"steps": [
[11, 5, 7, 14, 1, 0.3],
[20, 14, 34, 42, 0, 0.25],
[21, 15, 69, 77, 1, 0.03]
]
}
]